Application Note

PicoQuant

# Dual-Focus Fluorescence Correlation Spectroscopy

**Thomas Dertinger, University of California Los Angeles, USA**
**Benjamin Ewers, Benedikt Krämer, Felix Koberling, PicoQuant GmbH, Germany**
**Iris v. d. Hocht, Forschungszentrum Jülich, Germany**
**Jörg Enderlein, Georg-August-Universität Göttingen, Germany**

## Introduction

Fluorescence Correlation Spectroscopy (FCS) is a widely used tool to investigate the hydrodynamic properties of single molecules such as their diffusion coefficient and to study photophysical properties such as µs-blinking of fluorophores and antibunching. In FCS, the fluorescence intensity is correlated with a time shifted replica of itself for different time shifts (lag times) $\tau$ .

$$g(\tau)=\langle I(t+\tau)I(t)\rangle \qquad \textit{Eq. 1}$$

$I(t)$ is the fluorescence intensity at time $t$, $(t + \tau)$ is the fluorescence intensity at time $t + \tau$, and the triangular brackets denote averaging over all time values $t$. The physical meaning of this so called autocorrelation function is, that it is directly proportional to the probability to detect a photon at time $t + \tau$ if there was a photon detected at time $t$. If the detection volume is sufficiently small (~ femtoliter range) and the concentration of the fluorescent dye is sufficiently low (~ nanomolar range), the recorded fluorescence intensity is strongly fluctuating due to fluorescent dyes entering and exiting the detection volume as shown in Fig. 1.

These fluctuations are the basis of any autocorrelation analysis for which a typical result is shown in

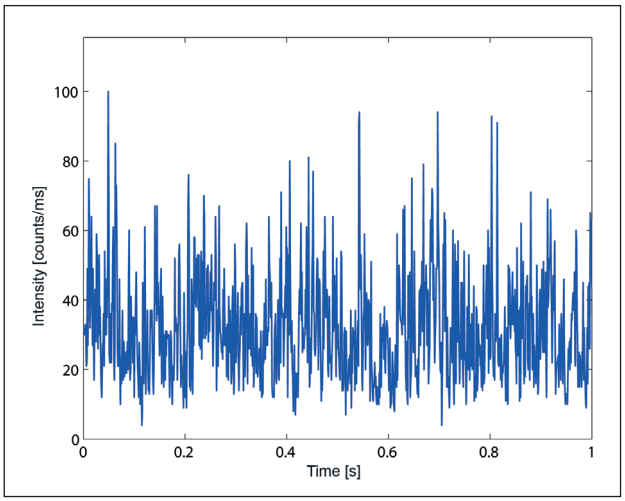


*Fig. 1: Typical intensity time trace as recorded with a confocal microscope. The signal fluctuations are due to fluorescent molecules which enter or leave the detection volume.*

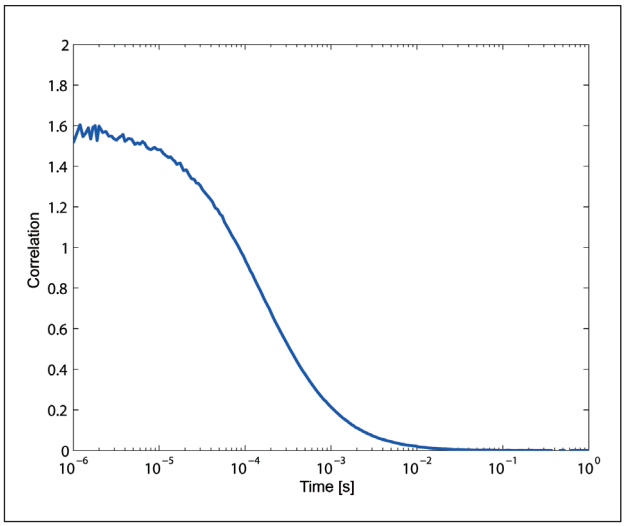


*Fig. 2: Typical autocorrelation curve measured with free diffusing Atto655 dye molecules (~ 5 nM) in aqueous solution.*

Fig. 2. To understand the shape of the autocorrelation curve let us consider the lag time dependence of $g(\tau)$: If a molecule is close to the centre of the detection volume, there will be a high probability to detect a large number of consecutive fluorescence photons from this molecule, i.e. the fluorescence signal will be highly correlated in time. When the molecule (due to diffusion) starts to exit the detection volume, this correlation will continually decrease in time, until the molecule has completely diffused out of the detection volume and the correlation is completely lost (correlation curve drops to zero). The faster a molecule diffuses, the faster the correlation will be lost. Thus, an autocorrelation analysis can provide information about the diffusion of fluorescing molecules, i.e. the diffusion coefficient. Any process which alters the diffusion coefficient can therefore be measured with FCS.

To quantitatively evaluate an FCS experiment, one has to exactly know the shape and the size of the detection volume, which is described by the so called molecule detection function (MDF) giving the probability to detect a fluorescence photon from a molecule at a given position in the sample space ([1], [2]). This MDF sensibly depends on manifold parameters of the optical set-up, which are difficult or sometimes even impossible to control. This makes an exact quantitative evaluation of an FCS measurements rather difficult. Refractive index mismatch of the sample solution and the objective's immersion medium, coverslide thickness variations and also laser beam properties such as astigmatism are parameters which influence the shape and size of the MDF and therefore the outcome of an FCS experiment. Especially the dependence of the MDF (and thus the FCS result) on optical saturation of the fluorescent dye, which can occur at even very low excitation powers of only a few µW, makes comparative measurements problematic. This is because the photophysics (and therefore the optical saturation properties) of even the same dye may change if it is bound to a target molecule [3].

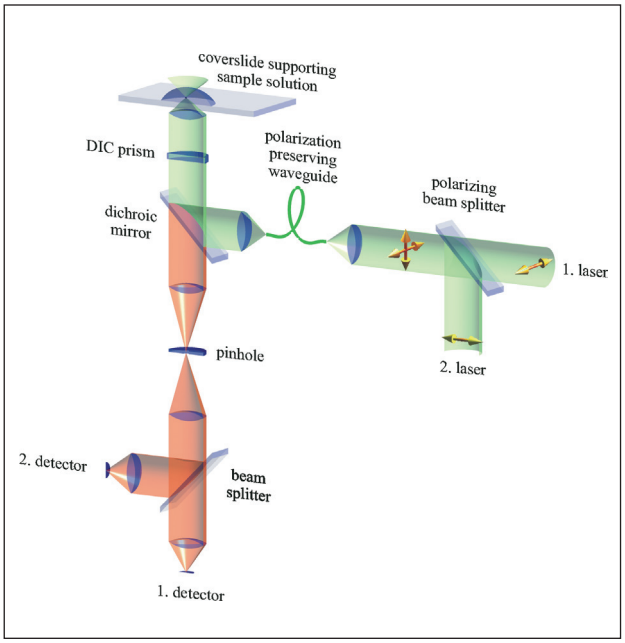


*Fig. 3: Schematic of the 2fFCS set-up.*

All these potential error sources are linked to one fundamental problem in conventional FCS – the absence of an intrinsic length scale in the measurement.

Recently, a new measurement scheme was developed, termed dual-focus-FCS (2fFCS), which is robust against the above mentioned potential error sources [4]. 2fFCS measures absolute values of diffusion coefficients without referencing against a sample with known diffusion coefficient, like it is often done in conventional FCS.

The core idea consists of two fundamental changes compared to conventional (single-focus) FCS:

1. The introduction of an external ruler into the measurement system by generating two laterally shifted but overlapping laser foci at a fixed and known distance.

2. These two foci and corresponding detection regions are generated in a way that the corresponding MDFs are sufficiently well described by a simple two-parameter model yielding accurate diffusion coefficients.

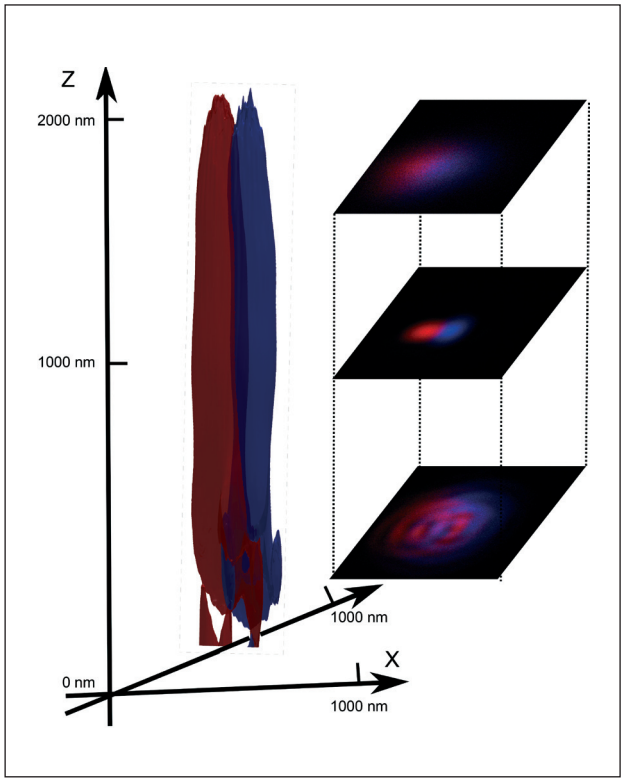


*Fig. 4: Measured 3D-isosurface ($1/e^2$) of the two overlapping PSFs of a typical 2fFCS set-up. The depicted volume is approximately 1-2 fl.*

## Set-up and working principle

The 2fFCS set-up used for this application note is based on a slightly modified MicroTime 200 confocal microscope (see Fig. 3 and 5). To generate the two shifted foci, two orthogonally polarized, pulsed diode lasers (LDH-P-C-640B) are combined with a polarization sensitive beamsplitter and afterwards coupled into a polarization maintaining single-mode fibre. At the fibre output the light is again collimated by an appropriate lens.

Both lasers are pulsed alternately (Pulsed Interleaved Excitation, PIE [5]). Alternate pulsing is accomplished by dedicated laser driver electronics (PDL 828 “Sepie II”). The combined light consists of a train of laser pulses with alternating orthogonal polarization. Before the objective the laser beam passes through a Nomarski prism (U-DICTHC, Olympus) that is normally exploited for differential interference contrast (DIC) microscopy. The principal axes of the Nomarski Prism are aligned with the orthogonal polarizations of the laser pulses, so that the prism deflects the laser pulses in two different directions according to their corresponding polarization. After focussing the light through the objective (UPLANAPO, 60x, water immersion, NA 1.2, Olympus), two overlapping excitation foci are generated with a small lateral shift between them (Fig. 4). The distance between the beams for a given wavelength is defined by the DIC prism and the objective. As long as these two elements are used, the distance will remain accurately constant over time. Fluorescence is collected by the same objective (epi-fluorescence set-up), passed through the DIC prism and the dichroic beamsplitter and is focussed into a single circular aperture (confocal pinhole). Behind the pinhole the light is collimated and divided by a non-polarizing beamsplitter cube and focussed onto two single-photon avalanche diodes. A Time-Correlated Single Photon Counting (TCSPC) unit (e.g. PicoHarp 300 or HydraHarp 400) is used for data acquisition, operating in the time-tagged time-resolved (TTTR) mode, which allows to record for every detected photon its arrival time with a temporal resolution in the nanosecond range (macroscopic time) and its arrival time with respect to the last laser pulse with picosecond timing resolution (TCSPC time).

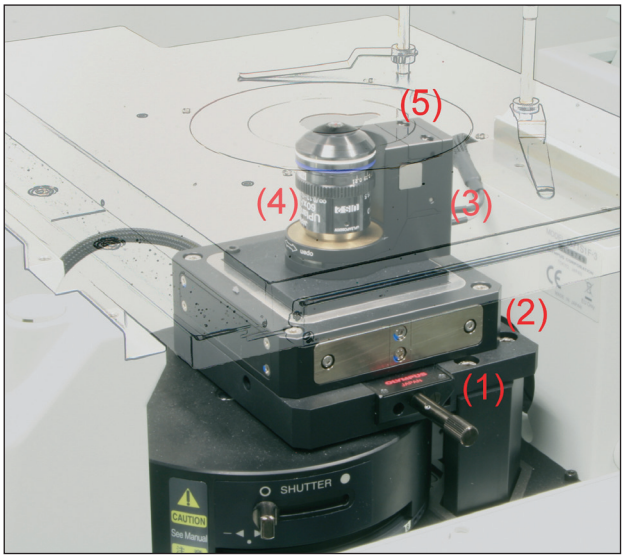


*Fig. 5: Setup of the MicroTime 200 with Nomarski prism (1), lateral scanner (2), axial scanner (3), objective (4) and sample stage (5).*

The TCSPC time of each recorded photon is used to determine in which laser focus/detection region the fluorescence light was generated.

A typical TCSPC histogram measured on an aqueous solution of Atto655 is shown in Fig. 6. The figure shows two time-shifted fluorescence decay curves (with a lifetime of approx. 2 ns) that correspond to the alternately pulsed lasers and two focal regions. Thus, for each laser focus the corresponding autocorrelation function can be calculated. However, in addition to the autocorrelation curves, one can also correlate the fluorescence signal from one laser focus with that of the second focus. By doing so, a cross-correlation curve is generated which is shifted to longer lag times and has a lower amplitude with respect to the auto-correlation curves (see Fig. 7, green curve). The shape of an autocorrelation curve is completely determined by the underlying MDF, whereas the shape of the cross-correlation curve is also dependent on the overlap of the two foci. If the distance between both lasers is known, a global fitting of both auto- and cross-correlation curves can yield the absolute diffusion coefficient. This is because the relative time shift between the cross correlation and auto correlation curves scales with the square of the foci distance divided by the diffusion coefficient. Moreover, the relation between cross-correlation and auto correlation amplitudes will be a direct measure for the focus overlap.

For fitting, a new semi-empirical MDF model has been developed by Jörg Enderlein [4]. Similar to the conventionally used 3D-Gauss-model the new model has also only two principal fit parameters. In contrast to the conventional Gauss-Model, however, the new model describes the underlying MDFs more accurate as has been shown in [4]. The focus shape is approximated with a scalar model for an diverging laser beam with a variable beam waist. This approach describes the MDFs much better than the assumption of a constant laser beam waist radius along the optical axis used in the conventional Gaussian model.

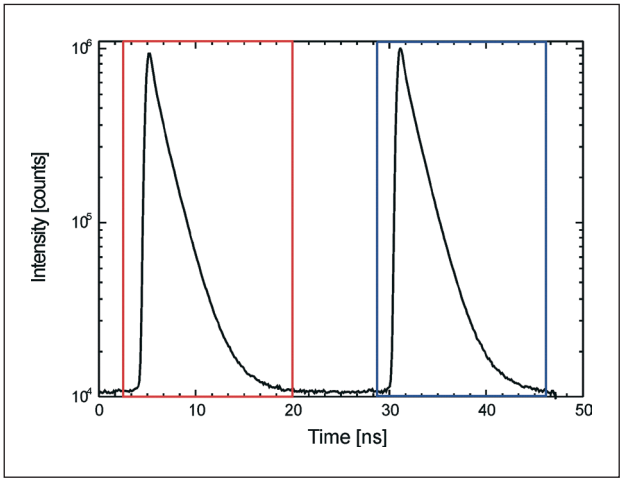


*Fig. 6: TCPSC histogram measured on an aqueous solution of Atto655. The photon counts in the left window (1.5 ns < t < 20 ns) are generated by the first laser, i.e. in the first focus. The photon counts in the right window (29 ns < t < 44 ns) are generated by the second laser corresponding to the second focus.*

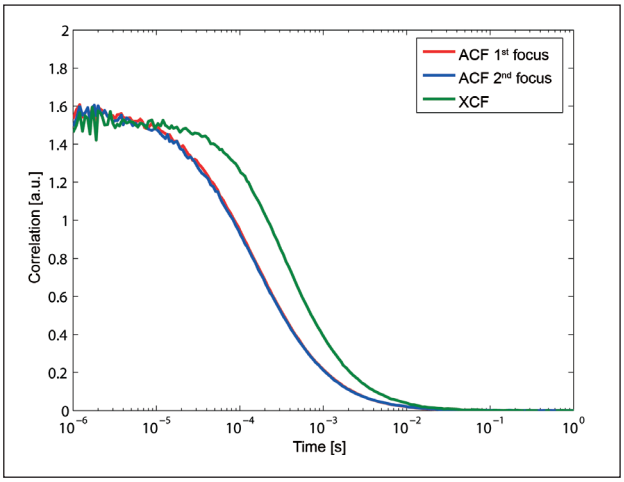


*Fig. 7: Typical auto (ACF) and cross (XCF) correlation curves recorded with the 2fFCS set-up. The two autocorrelation curves are almost identical whereas the cross-correlation curve is shifted to longer lag times. Note that the amplitude of the cross-correlation curve is multiplied by a factor of two in order to better visualize the lag time shift.*

# Results

### Determination of the inter-focal distance

In order to evaluate a 2fFCS measurement, it is essential to exactly determine the distance between the foci. One way to do this is to measure a substance with a known diffusion coefficient and to use the distance as a parameter in the corresponding fitting procedure of 2fFCS. For this purpose we have compiled a table listing diffusion coefficients of different fluorophors in water (see end of this publication).

An alternative and more direct approach would be to image the confocal volumes with 100 nm diameter fluorescent beads. This approach relies on the accuracy of the scanner which is in the case of the MicroTime 200 better than one nanometer. Such a scan is illustrated in Fig. 4. The interfocal distance can be determined by this technique with an accuracy of ± 4 % leading to an inaccuracy of ± 8 % of the diffusion coefficient.

### Optical saturation

In order to demonstrate the independence of the 2fFCS scheme against optical saturation, measurements of the diffusion coefficient of Atto655 in aqueous solution were carried out at different excitation intensities. As can be seen in Fig. 8 the diffusion coefficient remains constant up to an excitation intensity of approx. 40 µW. The subsequent rise in apparent diffusion coefficient at higher excitation powers is due to unavoidable photobleaching. The dye bleaches before it passes completely the second focus.

As a comparison the recorded data was also evaluated using only one autocorrelation curve, which corresponds to a conventional (single-focus) FCS set-up. Since conventional FCS measures only diffusion times and not diffusion coefficients, the data was evaluated using a standard model based on a three-dimensional Gaussian MDF and calibrated against the 2fFCS measurement. For the calibration it was assumed that the diffusion coefficients at zero excitation powers were equal for both methods. The corresponding correction factor for the conventional FCS data was thus determined by a linear extrapolation using the measurement data for excitation powers up to 35 µW.

As can be seen, there is a prominent decrease (up to 15 %) in the apparent diffusion coefficient (increase in diffusion times) using a conventional single-focus FCS approach. Since Atto655 has no triplet state, only excited state saturation can take place. For other red fluorescent dyes, which show triplet state dynamics (e.g. Cy5), the saturation effect might even be more pronounced.

### Refractive index mismatch

Measuring in solutions with a refractive index different to that of the objective's immersion medium is a potential error source in conventional FCS and leads to an increased diffusion time and thus to a decreased apparent diffusion coefficient. Such a refractive index mismatch is not a problem in a 2fFCS setup, which is shown by measurements of the diffusion coefficient of Atto655 in aqueous solutions containing different concentrations of guanidine hydrochloride (GdHCl). GdHCl, which is often used as denaturation reagent for protein folding experiments, increases not only the refractive index of the solution but also its viscosity. Using the Einstein-Stokes relation

$$D = \frac{k_B T}{6 \pi \eta r_H} \qquad \text{Eq. 2}$$

where $D$ denotes the diffusion coefficient, $k_B$ is the Boltzmann constant, $T$ the absolute temperature, $\eta$ the viscosity and $r_H$ the hydrodynamic radius, one would therefore, theoretically, expect a linear dependence of the diffusion coefficient with the inverse of the viscosity. The corresponding results of the 2fFCS measurements are shown in Fig. 9 and do very well reproduce this dependency. Furthermore the agreement between diffusion coefficients measured with 2fFCS and pulsed field gradient NMR experiments assures that also the absolute value of the diffusion coefficient is correct. It becomes also obvious that 2fFCS yields correct results even for large mismatches between the refractive index of the sample (n=1.44) and the refractive index of the objective's immersion medium (water, n=1.33).

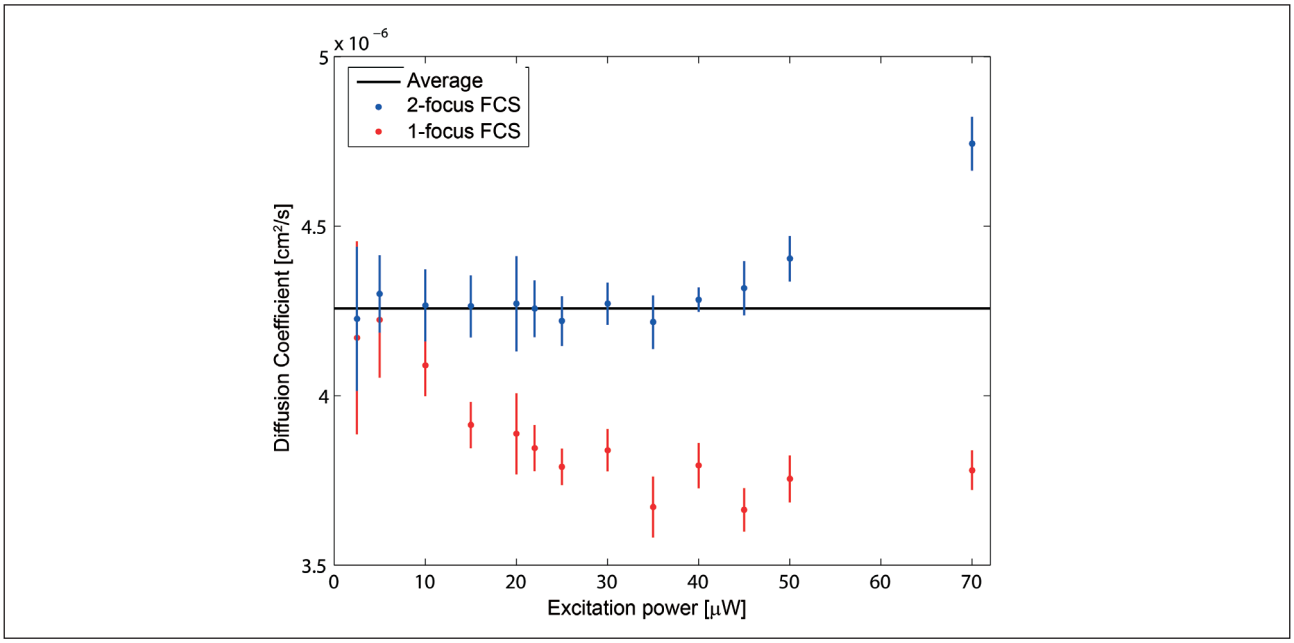


*Fig. 8: Measured diffusion coefficient of Atto655 in water at 25°C as a function of excitation power. The solid line is the mean value derived from the measurements at excitation powers up to 35 µW. As can be seen the values achieved with single focus FCS are decreasing as excitation power increases. At excitation powers higher than 40 µW photobleaching sets in and therefore the apparent diffusion coefficient becomes faster in 2fFCS whereas in 1fFCS the saturation effects are counterweighted by photobleaching.*

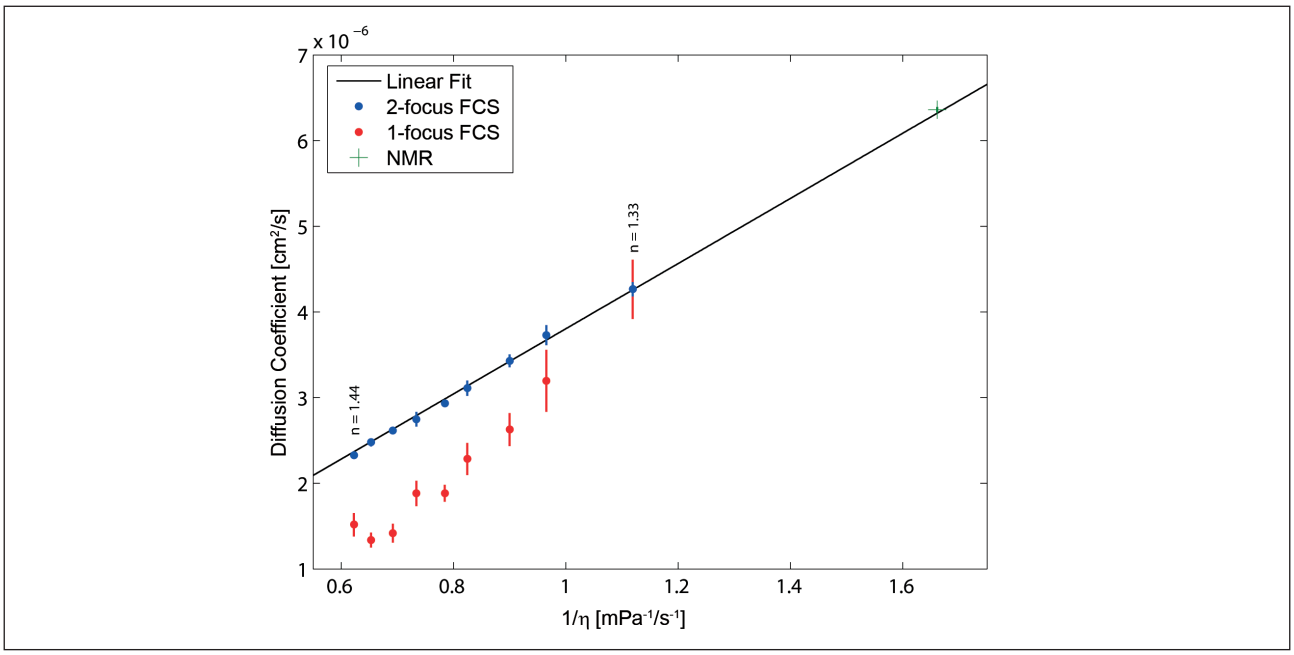


*Fig. 9: Dependence of the diffusion coefficient of Atto655 in aqueous GdHCl solution and deuterized methanol (D3COD) as a function of inverse viscosity. The solid line is a linear least square fit to all 2fFCS data (blue dots). Standard deviations are shown as error bars and are derived from ten repeated measurements (10 x 6 min). The green dot is derived from a pulsed-field gradient NMR experiment carried out in D3COD (rel. error 0.5 %). For comparison, the results achieved with single focus FCS are also shown (red dots).*

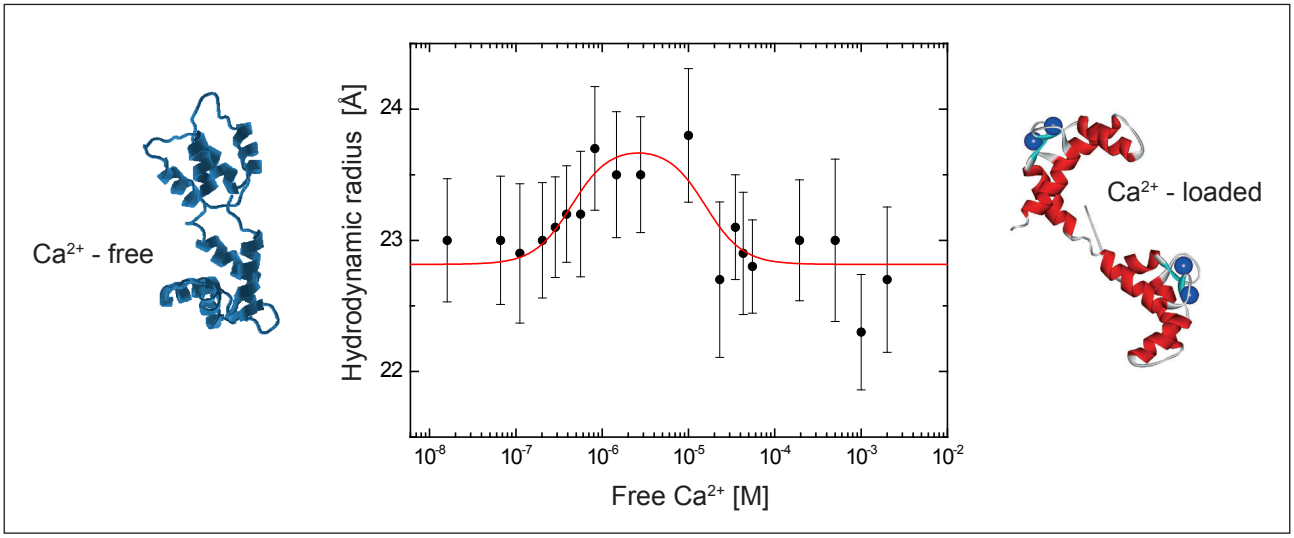


*Fig. 10: The Stokes radius of CaM labeled with Atto655 as a function of free calcium. The red line is a fit corresponding to a standard Hill Equation.*

As a comparison, the autocorrelation like in classical single focus FCS was also evaluated using a standard model based on a three-dimensional Gaussian MDF. The necessary values to correctly describe the focal volume in this fit were adapted in a way that the diffusion coefficients for Atto655 in pure water were equal for both methods. The results show deviations up to 35 % from the expected value and clearly demonstrate the high accuracy of 2fFCS compared to standard FCS measurements.

### Conformational changes of calmodulin

The big potential of 2fFCS can be demonstrated by the monitoring of the conformational change of calmodulin during calcium binding. CaM belongs to the family of calcium-binding proteins and is a key component of the calcium second messenger system. This small, acidic protein (~ 16.7 kD) is ubiquitous in all eukaryotic cells and can bind up to four calcium ions. To date the calcium loaded form is known to regulate the functions of about 100 diverse target enzymes and structural proteins [8, 9].

Several publications have found strong evidence that the transition between free (apo-) CaM and $Ca_4^{2+}$- CaM is a two step process [10]. It has been shown that half-saturated $Ca_4^{2+}$- CaM adopts an intermediate structure, which cannot be assigned to an average of both - the apo and the $Ca_4^{2+}$- CaM conformation [11]. However all evidence for a global structural change is based on data coming from single structural elements of CaM, which makes drawing conclusions of these observations difficult.

In the following the Stokes radius is measured as a function of the free calcium concentration. The results give direct evidence to the existence of an intermediate $Ca_2^{2+}$- CaM conformation and prove that 2fFCS is able to monitor smallest changes in hydrodynamic properties of bio-molecules.

The diffusion coefficient of Atto655 labeled CaM at different calcium concentrations was measured with 2fFCS at 25°C. For the whole set of measurements the corresponding Stokes radii were derived from the estimated diffusion coefficients and are shown in Fig. 10 as a function of the free calcium concentration.

At very low calcium concentrations (16 nM) CaM is in the apo-conformation, whereas at high calcium concentrations (0.5 - 2 mM), CaM is calcium saturated and adopts the $Ca_4^{2+}$- conformation. Between the apo- and the $Ca_4^{2+}$- conformation a rise in Stokes radius of up to 23.7 Å at 3 µM free calcium can be observed. This rise in Stokes radius is attributed to a conformational change of CaM upon calcium binding and an associated rearrangement of the hydration layer. Above 3 µM, the Stokes radius is decreasing down to 22.8 Å. Since the calcium binding constants range from 0.2 µM to 40 µM under comparable conditions [12], it is likely that we monitor an intermediate conformation of CaM where only some of the binding sites are occupied by calcium ions, but not all. Comparing the observed biphasic behaviour with published results, it is most likely that this change in conformation can be attributed to the formation of $Ca_2^{2+}$- CaM. NMR studies find that major changes in chemical shifts are taking place only when CaM has bound 0, 2 or 4 calcium ions, whereas the binding of the first and the third ion does not induce large changes in protein structure [13].

### Conclusion

It has been shown that 2fFCS is robust against typical artefacts conventional (single-focus) FCS is prone to. In addition to its numerous advantages over conventional FCS, upgrading a MicroTime 200 micro-

scope to a 2fFCS system is surprisingly easy. The method has proved to be relatively robust against misalignments of the system. The 2fFCS analysis is, however, not part of the MicroTime 200 software SymPhoTime but can be obtained as a MATLAB® [8] script.

Standard laser scanning microscopes cannot be easily upgraded to 2fFCS functionality because of polarizing elements in the beam path and the wrong angle under which the DIC prism is placed.

2fFCS is a true single molecule technique which enables the user to measure at very low concentrations, which are often necessary in order to avoid aggregation of proteins or other biomolecules (e.g. during unfolding experiments under denaturing conditions). This feature makes 2fFCS superior to other methods for measuring the diffusion coefficient such as dynamic light scattering or gel permeation chromatography, which fail to measure at nanomolar analyte concentrations. However, the applicable concentration range is constricted from 0.1 pM up to 5 nM (10 pM up to 50 nM for standard FCS) since the size of the confocal volume is bigger compared to conventional FCS. This can pose a limitation to measurements in living cells.

The measurements show that small changes even below one Angstrøm can be monitored with 2fFCS. This sensitivity is unique for a measurement at these low concentrations and under native conditions. Dual-focus FCS opens up a new window for this kind of investigations.

**Additional sample information**

Atto655-(COOH) was purchased from Atto-Tec GmbH Germany. Guanidine hydrochloride was purchased from Sigma-Aldrich. Alexa647-maleimide was purchased from Invitrogen, Karlsruhe, Germany. CaM was labeled nonspecifically with NHS-functionalized red fluorescent dye Atto655. Each measurement lasted for 10 min, and for each calcium concentration, measurements were repeated several times on different days to determine a standard deviation for the diffusion coefficient.

| Fluorophore | $\lambda_{Em}$ maximum in nm | Diffusion coefficient in water **at 25°C (298.15 K)** in $10^{-6}$ $cm^2s^{-1}$ | Methods |
|---|---|---|---|
| Atto655-maleimid | 686 | 4.07 ± 0.10<br>4.06 ± 0.09<br>4.09 ± 0.07 | 2fFCS, PFG-NMR<br>2fFCS<br>pmFCS |
| Atto655-carboxylic acid | 685 | 4.26 ±0.08 | 2fFCS, PFG-NMR |
| Atto655-NHS esther | 685 | 4.25 ± 0.06 | 2fFCS |
| Cy5 | 670 | 3.6 ± 0.1 | 2fFCS |
| Alexa 647 | 665 | 3.3 ± 0.1 | 2fFCS |
| Alexa 633 | 647 | 3.4 ± 0.1 | 2fFCS |
| Rhodamine 6G | 550 | 4.14 ± 0.05<br>4.3 ± 0.4<br>4.14 ± 0.01 | 2fFCS<br>PFG-NMR<br>PB/CF |
| Rhodamine B | 560 | 4.5 ± 0.4<br>4.27± 0.04 | PFG-NMR<br>PB/CF |
| Rhodamine 123 | 530 | 4.6 ± 0.4 | PFG-NMR |
| Rhodamine 110 | 535 | 4.7 ± 0.4 | PFG-NMR |
| Fluorescein | 520 | 4.25 ± 0.01 | PB/CF |
| Oregon Green 488 | 550 | 4.11 ± 0.06<br>4.± 0.08 | 2fFCS<br>2fFCS |
| Atto488-carboxylic acid | 523 | 4.0 ± 0.1 | 2fFCS |
| TetraSpeck Beads, 0.1µm diameter | 430<br>515<br>580<br>680 | 0.044 ± 0.07 | 2fFCS, DLS |

*Table taken from http://www.picoquant.com/technotes/appnote_diffusion_coefficients.pdf*

*Abbreviations of measurement methods:*
*2fFCS, Dual Focus Fluorescence Correlation Spectroscopy; PFG-NMR, Pulsed Field Gradient Nuclear Magnetic Resonance; pmFCS, Polarization-Modulation Fluorescence Correlation Spectroscopy; PB/CF, Plug Broadening/Capillary Flow; DLS, Dynamic Light Scattering.*

# References

[1] Enderlein, J., Gregor, I. , Patra, D., Fitter, J., Curr. Pharm. Biotechnol. , Vol. 5, p. 155-161 (2004)

[2] Gregor, I., Enderlein, J., Opt. Lett, Vol. 30, p. 2527 – 2529 (2005)

[3] Enderlein, J., Gregor, I., Patra, D., Dertinger, T., Kaupp, U. B., ChemPhysChem, Vol. 6, p. 2324 – 2336 (2005)

[4] Dertinger, T., Pacheco, V., von der Hocht, I., Hartmann, R., Gregor, I., Enderlein, J., ChemPhysChem, Vol. 8, p. 433 – 443 (2007)

[5] Müller, B. K., Zaychikov, E., Bräuchle, Ch., Lamb, D. C., Biophysical J. Vol. 89, p. 3508 – 3522 (2005)

[6] Benda, A., Benes, M., Marecek, V., Lhotsky, A., Hermens, W. T., Hof, M., Langmuir, Vol. 19, p. 4120 – 4126 (2003)

[7] Senin, I. I., Fischer, T., Komolov, K. E., Zinchenko, D. V., Philippov, P. P., Koch, K. W., J. Biol. Chem., Vol. 277, p. 50365 – 50372 (2002)

[8] O'Neil, K.T., DeGrado, W. F.,Trends in Biochemical Sciences, 15, 59-64 (1990)

[9] Crivici, A., Ikura, M., Annu. Rev. Biophys. Biomol. Struct., 24, 85-116 (1995)

[10] Grabarek, Z., J. Mol. Biol., 346, 1351-1366 (2005)

[11] Shea, M. A., Verhoeven, A. S., Pedigo, S., Biochemistry, 35, 2943-2957 (1996)

[12] Linse, S., Helmersson, A., Forsen, S., Journal of Biological Chemistry, 266, 8050-8054 (1991)

[13] Seamon, K. B., Biochemistry, 19, 207-215 (1980)

[14] MATLAB® http://www.mathworks.de/products/matlab/

PicoQuant GmbH
Rudower Chaussee 29 (IGZ)
12489 Berlin
Germany

Phone +49-(0)30-6392-6929
Fax +49-(0)30-6392-6561
Email info@picoquant.com
WWW http://www.picoquant.com